# Reducing Bit Error Rate with Optical Phase Regeneration in Multilevel Modulation Formats

**Graham Hesketh, Peter Horak**
*Optoelectronics Research Centre, University of Southampton, Southampton, SO17 1BJ, UK*
** Corresponding author: gdh1e10@soton.ac.uk*

Received Month X, XXXX; revised Month X, XXXX; accepted Month X, XXXX; posted Month X, XXXX (Doc. ID XXXXX); published Month X, XXXX

We investigate theoretically the benefits of using all-optical phase regeneration in a long-haul fiber optic link. We also introduce a design for a device capable of phase regeneration without phase-to-amplitude noise conversion. We simulate numerically the bit-error rate of a WDM optical communication system over many fiber spans with periodic re-amplification and compare the results obtained with and without phase regeneration at half the transmission distance when using the new design or an existing design. Depending on the modulation format, our results suggest that all-optical phase regeneration can reduce the bit-error rate by up to two orders of magnitude and that the amplitude preserving design offers a 50% reduction in bit-error rate relative to existing technology. 
*OCIS Codes: 060.2330, 060.1155, 230.1150, 230.432*

All-optical phase regeneration of fiber optic communication signals has been proposed to reduce the impact of phase noise induced by, e.g., amplified spontaneous emission (ASE) in amplifiers or nonlinear self/cross-phase modulation (S/XPM) and four wave mixing (FWM) of pulses during transmission in a multi-user wavelength division multiplexed (WDM) system. By regenerating at a distance prior to which few or no errors have occurred, the signal can subsequently be transmitted further for the same bit error rate (BER). Optical phase regeneration has been experimentally demonstrated for 2 [1,2] and 4 [3-5] phase levels and in principle extends to higher level phase shift keying formats [3,5] where greater spectral efficiency is offered. At high bit rates optical regeneration may work faster and consume less power than electronic compensation and its fiber-to-fiber nature offers simple network integration [6].

The phase regeneration method in [3-5] utilizes FWM in a highly nonlinear fiber (HNLF) to realise a staircase in the phase of the following signal transfer function [blue-dashed line, Fig.1, a)]:

$$A_{out}e^{i\phi_{out}} \propto e^{i\phi_{in}} + m_1 e^{-i(M-1)\phi_{in}}, \qquad (1)$$

where $A$ and $\phi$ are the signal electric field amplitude and phase respectively, $M$ is the integer phase quantization number and $m_1$ is the phase harmonic weight. The step function maps all input phase samples falling within the width of the step to a single output phase, the height of the step. However, while Eq. (1) is excellent at squeezing phases to desired constellation points, it suffers notable phase-to-amplitude noise conversion as the output amplitude oscillates as a function of input phase [blue-dashed line, Fig.1 b)]. Additional amplitude noise is undesirable in phase shift keying formats as it converts back into phase noise during subsequent propagation. While phase regeneration has been demonstrated [3-5], the impact of this feature on the BER of a long-haul communication link has not yet been investigated. Amplitude noise is even more undesirable in phase and amplitude keying formats as it leads directly to bit errors.

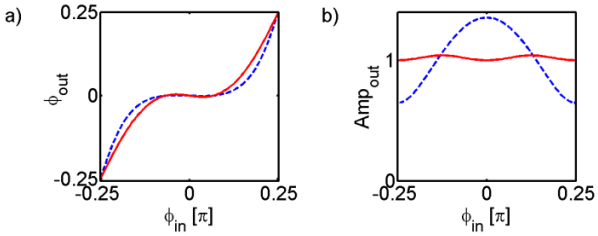


Fig. 1. a) Phase, b) amplitude transfer as a function of signal input phase [blue-dashed line, Eq. (1): $m_1 = 0.33$, $M = 4$, red-solid line, Eq. (2): $m_2 = 0.14$, $M = 4$]; in Eq. (2) the amplitude is flat for a small sacrifice in the phase step width.

The purpose of this paper is twofold. Firstly, we introduce the following modification to Eq. (1):

$$A_{out}e^{i\phi_{out}} \propto e^{i\phi_{in}} + m_2 e^{-i(M-1)\phi_{in}} - m_2 e^{i(M+1)\phi_{in}}. \qquad (2)$$

The opposing signs of harmonic weights in Eq. (2) cause the amplitude response of the harmonics to interfere destructively while their phase responses combine constructively. This maintains the phase step while the amplitude becomes flat (red-solid line, Fig.1) enabling phase regeneration without phase to amplitude noise conversion. Secondly, a realistic BER simulation in a WDM system is presented which, for the first time, estimates the impact phase regeneration has on the BER. In some experiments the noise is artificially created and its distribution biased to supply more phase noise than amplitude noise [2, 4]. Such noise distributions are useful for demonstration purposes but are not necessarily realistic representations of noise in modern day fiber communications when WDM is employed [7]. With multiple channels and multiple sources of noise, amplitude noise and phase noise are often comparable [8]. It is thus imperative that optical regeneration is demonstrated in a state of the art communications scenario if it is to be championed as viable there. The BER simulation also enables future comparisons with other methods involving nonlinear amplifying loop mirrors [9] or a superposition of phase conjugated twin waves [10].

Fig. 2 shows the black box regenerator we simulate to regenerate a demultiplexed signal mid-link; it is similar in design to those experimentally verified [2-5] and our specific modifications for Eq. (2) our highlighted in red. The signal enters HNLF 1 together with a portion of a local pump P1 (frequency offset by $\Delta f$ ) [HNLF (1 and 2) parameters: $L$=300 m, nonlinear coeff. $\gamma$=11 W$^{-1}$km$^{-1}$, dispersion $D(\lambda$=1555.6 nm) = -0.8 ps/(km.nm) , dispersion slope $S = 0.018$ ps/(km.nm$^2$), loss $\alpha = 0.2$ dB/km ]. This generates cascaded FWM harmonics at multiples of $\Delta f$ , each carrying a multiple of the signal phase due to phase conservation. Two of these, which fall at multiples of $M\Delta f$ , are modulation free [2] and are used as pumps P2 and P3. They are isolated by a wavelength selective switch (WSS) and amplified through opto-injection locking (OIL), while the signal and harmonics are directed through a separate fiber. Piezo fiber stretchers (PZTs), can be used to counteract slow thermal and acoustic phase drifts [2-5] and to ensure that all waves remain phase locked at this stage; PZT 1 suffices to maintain the appropriate relative phases in Eq. 1, while PZT 2 is also required for the third term in Eq. 2. Pumps P1, P2 and P3 meet together with the signal and harmonics in HNLF 2 [Fig. 2 b)] where non-degenerate FWM takes phase conjugated photons from the harmonics to the signal frequency, realising Eq. (1) or (2). The harmonic weights $m_i$ $(i = 1,2)$ in Eqs. (1) and (2) are tuned by adjusting pump powers. Finally the signal is properly filtered and assessed. In addition to these methods, we also note an alternative dual-conjugated-pump degenerate scheme has been considered [11, 12] with the advantage of reduced spectral harmonic separation and that two frequency channels have been phase regenerated simultaneously [13]. Furthermore, periodically poled lithium niobate (PPLN) waveguides have been considered as a promising more compact alternative to HNLFs [14, 15].

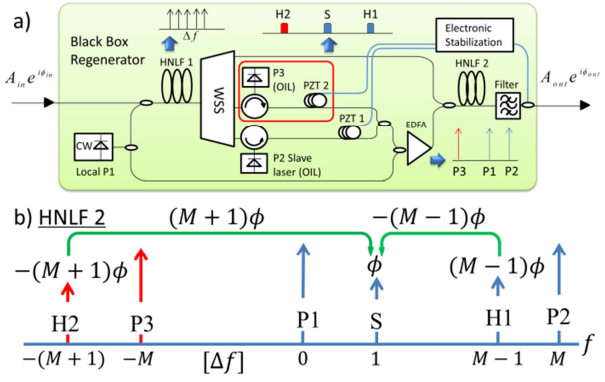


Fig. 2. a) Proposed regenerator. b) FWM of harmonics (H), signal (S) and pumps (P) in HNLF 2. [a), b) red highlights for Eq. (2)].

First, we simulated the HNLF sections of the regenerator in full to prove that, by carefully tuning the pump powers, we were able to perfectly match the analytic transfer functions, Eq. (1) and (2). Having done so, to save computation time the analytic functions were used for the regenerator section in all BER tests presented hereafter. To optimize $m_i$, the process in [5] was used as a guide and fine-tuned to improve BER.

To simulate long haul transmission for the BER tests, a generalised nonlinear Schrödinger equation [16] incorporating nonlinear and dispersive interactions was solved numerically using a split-step Fourier method. Gaussian pulses modulated with Gray coded Q-PSK, 8-PSK and star 8-QAM data, were frequency multiplexed over 51 multi-user channels separated by 75 GHz about a central wavelength of $\lambda$=1555.6 nm with a symbol rate of 13.33 GBaud giving a channel bit-rate of 26.6 Gbits/s for Q-PSK (2 bits/symb.) and 40 Gbits/s for 8-PSK and star 8-QAM (3 bits/symb.). Each channel was narrowly filtered at the transmitter using a super Gaussian filter to isolate the central spectral lobe. While this introduces some inter-symbol interference it ultimately reduces the BER when the same filter is used to demultiplex before the regenerator and again at the receiver as it reduces power in low signal-to-noise ratio spectral regions allowing an increase in total average power and improved signal-to-noise ratio. For transmission, a standard single-mode communications fiber was used with single span length $L$=100 km, nonlinear coefficient $\gamma$=1.3 W$^{-1}$km$^{-1}$, dispersion $D = 16.8$ ps/(km.nm) at $\lambda$=1555.6 nm, dispersion slope $S = -41.55$ ps/(km.nm$^2$), and loss $\alpha = 0.18$ dB/km and a short dispersion compensating fiber section was simulated in every span [17]. After each span the average peak power was restored using amplification with a 3 dB noise figure. At mid-link, each channel was isolated and regenerated as discussed above, then recombined for further propagation. After simulating the remaining transmission, frequency demultiplexing, sampling and mean phase error correction were performed before the bit errors were counted.

To calculate the BER, $2^7 = 128$ symbols were propagated in each of the 51 channels; the temporal and spectral simulation windows determined the trade-off between channel number and pulse repetition rate. Average peak pulse power was swept and each simulation was repeated 20 times at each power level on a supercomputer using different random input sequences. Consequently, combining all the data from all channels meant a single error corresponded to a BER of $\sim 1\times10^{-6}$ in all modulation formats, which is to be compared with the $1\times10^{-3}$ BER required to enable forward error correction (FEC); propagation distances were selected to yield a BER approaching the FEC limit without regeneration. The BER was found by comparing the known binary input sequences with output sequences obtained by decoding via the solid-black line decision thresholds in Fig 3-5, a)-c).

We first considered Q-PSK data ($M = 4$). Figs. 3 a)-c) indicate the noise distribution in constellation diagrams formed by combing all the electric field pulse-peak signal samples from all channels. Each diagram was plotted at the respective optimal power level as determined by the minimum BER, Fig. 3 f). The colours indicate sample density; a 200×200 square grid was fitted to the plotting area and samples per grid square were counted [colours map linearly across the density range of the bottom row, the same map is also used in the top row where any density above the last value in the colorbar appears red]. We compared the BER after filtering alone (demultiplexing) at the halfway stage [13 spans] and

recombining having bypassed the phase regenerator [Fig. 3 a) and black-circle-lines Figs. d)-f)], with filtering and phase regenerating using Eq. (1) with $m_1 = 0.33$, [Fig. 3 b) and blue-triangle lines Figs. d)-f)], and with phase regeneration using Eq. (2) with $m_2 = 0.14$, [Fig. 3 c) and red-square lines Figs. d)-f)]. Fig. 3 a) top is also indicative of the noisy signal prior to regeneration and b) and c) are indicative of post regeneration; the amplitude preserving case c) can be seen to exhibit a small amount of residual phase noise compared to b), due to the small reduction in phase step size but c) is also more concentrated in amplitude. Likewise, in Fig. 3 d), the phase variances after regeneration at the halfway stage are seen to be comparable in both regenerative designs and are considerably less than the bypassed case, while the amplitude variance after regeneration in Eq. (2) is identical to the bypassed case, while for Eq. (1) amplitude variance increases relative to the bypass case. As indicated in the bottom row of Figs. 3 a)-c) and e), both Eq. (1) and (2) reduce phase noise at the end of the link relative to the bypass case but to compare designs there the most useful figure is the BER in Fig. f).

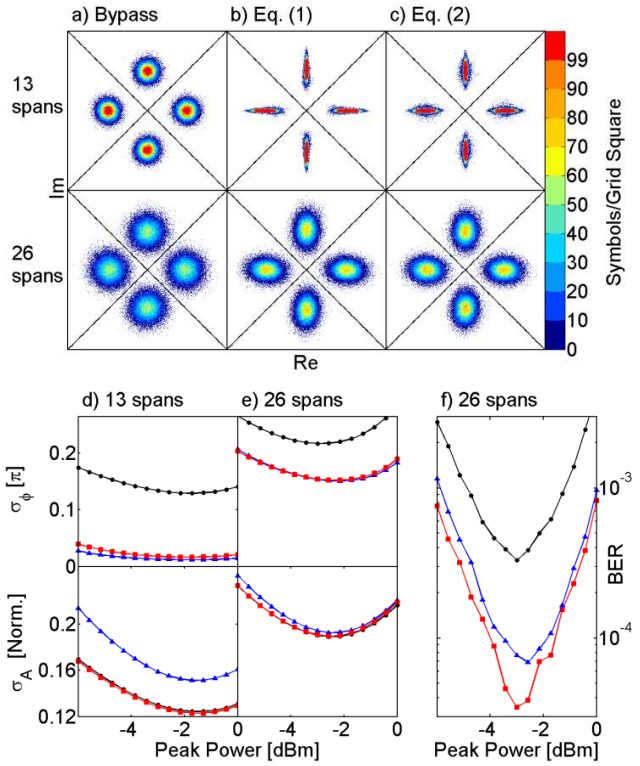


Fig. 3. a), b), c): Q-PSK constellation diagrams at -3, -2.57 and -3 dBm respectively (top row: post regeneration). d), e): phase and normalized amplitude error variances, [black-circle: bypass, blue-triangle: Eq. (1), red-square: Eq. (2)]. f): Corresponding bit-error rate. [ Eq. (1): $m_1 = 0.33$, Eq. (2): $m_2 = 0.14$ ].

Without regeneration the BER reached the $1\times10^{-3}$ FEC limit at 2600 km, with a minimum BER of $0.33\times10^{-3}$ at optimal input peak power -3 dBm. At this distance, mid-link regenerating using Eq. (1) with $m_1 = 0.33$ reduces the minimum BER at 26 spans to $0.69\times10^{-4}$ at -2.57 dBm and regenerating using Eq. (2) with $m_2 = 0.14$ reduces the minimum BER to $0.35\times10^{-4}$ at -3 dBm. The amplitude preserving Eq. (2) thus reduces the BER by ~1 order of magnitude in comparison to the bypass case and it offers a 50% reduction in BER relative to Eq. (1). Eq. (2) reduces the optimum BER relative to Eq. (1) because in Eq. (1) symbols pushed to low amplitude in the regenerator suffer more from ASE noise in subsequent propagation and bits pushed to high amplitude suffer more from XPM and FWM. In the amplitude preserving case, more symbols travel at the optimal power level (the minimum of the BER curves) which minimizes phase noise and errors. In Fig. 3 e) bottom, the amplitude variance curves are seen to almost coalesce at the end of the link. This suggests the extra amplitude variation induced by Eq. (1) doesn't survive to the end of the link, perhaps because large amplitude pulses pump low amplitude pulses in neighbouring channels, but none the less there is a substantial difference in the BER.

Next, we investigate 8-PSK ($M = 8$, Fig. 4). This format was less robust to noise than Q-PSK which meant that without regeneration the BER approached the $1\times10^{-3}$ FEC limit at just 1300 km with a minimum BER of $0.97\times10^{-3}$ at optimal input peak power -1.6 dBm.

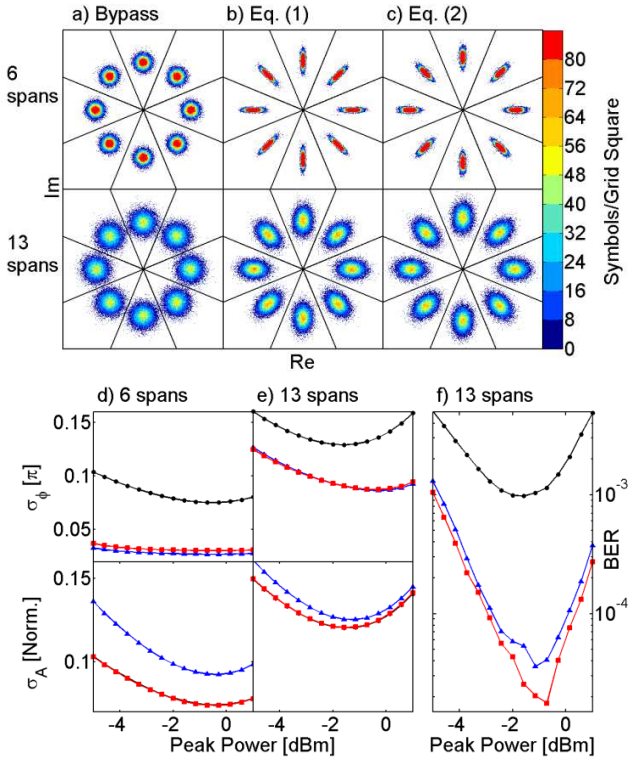


Fig.4. a), b), c): 8-PSK constellation diagrams at -1.6, -1.14 and -0.71 dBm respectively (top row: post regeneration). d), e): phase and normalized amplitude error variances, [black-circle: bypass, blue-triangle: Eq. (1), red-square: Eq. (2)]. f): Corresponding bit-error rate.[Eq. (1): $m_1 = 0.22$, Eq. (2): $m_2 = 0.1$ ].

Regenerating at 600 km using Eq. (1) with $m_1 = 0.22$ reduces the minimum BER at 1300 km to $0.36\times10^{-4}$ at -1.14 dBm and regenerating at 600 km using Eq. (2) with $m_2 = 0.1$ reduces the minimum BER at 1300 km to $0.18\times10^{-4}$ at -0.71 dBm. Thus, in the 8-PSK format Eq. (2) reduces the BER by ~2 orders of magnitude in comparison to the bypassed case and Eq. (2) offers a 50%

reduction in BER in comparison to Eq. (1), just like for Q-PSK. Phase regeneration has had more of an impact in this format due to a reduction in the phase dimension of the decision area. Once again the constellation diagrams Fig 4. a)-c), and the phase and amplitude variances Fig 4. d) and e) respectively, show the ability of Eq. (2) to perform phase regeneration without phase to amplitude noise conversion with the variances showing similar traits to the Q-PSK case. While the impact of regeneration is particularly impressive in this format, the larger $M$ is a disadvantage as it increases the spectral separation of the harmonics making them harder to generate in the first HNLF as more cascaded FWM processes are required to reach distant harmonics.

Finally, we consider star 8-QAM (Fig. 5) which also sends 3 bits/symbol but in an alternative way to 8-PSK.

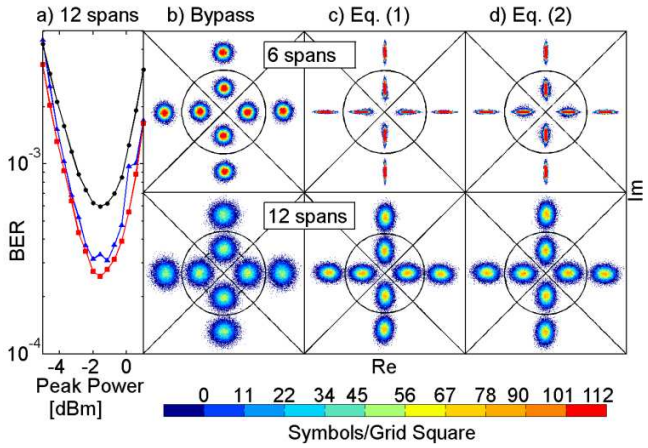


Fig. 5. a) Star 8-QAM bit error rate [black-circle: bypass, blue-triangle: Eq. (1), red-square: Eq. (2)]; phase/amplitude error variances omitted for clarity. b), c), d) constellation diagrams at -1.57, -1.14 and -1.57 dBm respectively, (top row: post regeneration). Parameters: Eq. (1): $m_1 = 0.33$ , Eq. (2): $m_2 = 0.14$ .

Without regeneration the BER approaches the FEC limit at approximately 1200 km with a minimum BER of $0.6\times10^{-3}$ at optimal input peak power -1.57 dBm. Regenerating at 600 km using Eq. (1) with $m_1 = 0.33$ reduces the minimum BER at 1200 km to $0.31\times10^{-3}$ at -1.14 dBm while regenerating using Eq. (2) with $m_2 = 0.14$ reduces the minimum BER at 1200 km to $0.25\times10^{-3}$ at -1.57 dBm. Thus, in the star 8-QAM format Eq. (2) yields a BER that is 43% of the BER in the bypassed case and 82% of the BER obtained with Eq. (1). Phase regeneration has had less of an impact in this format as amplitude noise remains uncorrected and contributes to bit errors. For star 8-QAM we thus suggest that an amplitude regenerator, e.g. [9], may also be required to achieve larger BER improvements. Note that, for a fair comparison, the amplitude level ratio was independently optimized in each design; the inner level was 0.41, 0.4 and 0.37 times the outer level value in the bypass, Eq. (1) and Eq. (2) cases respectively. Furthermore, at the transmitter the outer level was rotated relative to the inner to counteract the relative rotation due to SPM, although the offset was negligible for peak powers below 0 dBm. Lining up the amplitude levels at the regenerator improves performance but could only be done at the transmitter or at an electronic regenerator which limits this format at peak powers above 0 dBm. In contrast, this format uses $M = 4$ and not $M = 8$ which simplifies the generation of harmonics in the regenerator.

In summary, we proposed a design for an all optical phase regenerator that preserves the amplitude. By simulating both a previously demonstrated design and the amplitude preserving design in 3 modulation formats we showed that the BER can be reduced by as much as 2 orders of magnitude after regenerating mid-link, subject to modulation format. The new design offers a 50% reduction in BER relative to existing laboratory technology and could ultimately lead to cheaper and greener all-optical fiber communication networks.

This work was supported by the EPSRC research grant EP/J012874 and we thank Liam Jones, Kyle Bottrill, Francesca Parmigiani, Periklis Petropoulos and David Richardson for useful discussions.

## References


1. K. Croussore, I. Kim, Y. Han, C. Kim, G. Li, and S. Radic Opt. Express, **13** (11), 3945 (2005).
2. R. Slavík, F. Parmigiani, J. Kakande, C. Lundström, M. Sjödin, P. A. Andrekson, R. Weerasuriya, S. Sygletos, A. D. Ellis, L. Grüner-Nielsen, D. Jakobsen, S. Herstrøm, R. Phelan, J. O'Gorman, A. Bogris, D. Syvridis, S. Dasgupta, P. Petropoulos and D. J. Richardson, Nature Photon., **4**, 690 (2010).
3. J. Kakande, R. Slavík, F. Parmigiani, A. Bogris, D. Syvridis, L. Grüner-Nielsen, R. Phelan, P. Petropoulos and D. J. Richardson, Nature Photon., **5,** 748 (2011).
4. J. Kakande, A. Bogris, R. Slavík, F. Parmigiani, D. Syvridis, M. Sköld, M. Westlund, P. Petropoulos, and D. J. Richardson, OFC/NFOEC OMT4, (2011).
5. J. Kakande, R. Slavik, F. Parmigiani, P. Petropoulos and D. J. Richardson, OFC/NFOEC OW1I.3, (2012).
6. Z. Zhu, X. Chen, F. Ji, L. Zhang, F. Farahmand and J. P. Jue, J. Lightwave Technol., **30** (19), 3147 (2012).
7. P. Minzioni, V. Pusino, I. Cristiani, L. Marazzi, M. Martinelli and V. Degiorgio, IEEE Photonics Journal, **2** (3), 284 (2010).
8. D. Lavery, C. Behrens and S. J. Savory, Opt. Express, **19** (26), B836-B841 (2011).
9. K. Cvecek, K. Sponsel, G. Onishchukov, B. Schmauss, and G. Leuchs, IEEE Photon. Technol. Lett., **19** (3), 146 (2007).
10. X. Liu, A. R. Chraplyvy, P. J. Winzer, R. W. Tkach and S. Chandrasekhar, Nature Photon., **7**, 560 (2013).
11. J. Yang, Y. Akasaka and M. Sekiyaet, ECOC P3.07, (2012).
12. B. Stiller, G. Onishchukov, B. Schmauss and G. Leuchs, CLEO Munich CI-P.14 (2013).
13. S. Sygletos, P. Frascella, S. K. Ibrahim, L. Grüner-Nielsen, R. Phelan, J. O'Gorman, and A. D. Ellis, Opt. Express, **19** (26), B938 (2011).
14. K.J.Lee, F.Parmigiani, S.Liu, J.Kakande, P.Petropoulos, K.Gallo, D.J.Richardson, Opt. Express, **17** (22), 20393 (2009).
15. T. Umeki, M. Asobe and H. Takenouchi, Opt. Express, **21** (10), 12077 (2013).
16. R. Essiambre, G. J. Foschini, G. Kramer, P. J. Winzer, Phys. Rev. Lett., **101**, 163901 (2008).
17. K. Thyagarajan and B. P. Pal, J. Opt. Fiber. Commun. Rep., **4** (3), 173 (2007).

**Full References**


1. Kevin Croussore, Inwoong Kim, Yan Han, Cheolhwan Kim, Guifang Li, and Stojan Radic, "*Demonstration of phase-regeneration of DPSK signals based on phase-sensitive amplification*", Optics Express, **13** (11), 3945-3950 (2005).

2. Radan Slavík, Francesca Parmigiani, Joseph Kakande, Carl Lundström, Martin Sjödin, Peter A. Andrekson, Ruwan Weerasuriya, Stylianos Sygletos, Andrew D. Ellis, Lars Grüner-Nielsen, Dan Jakobsen, Søren Herstrøm, Richard Phelan, James O'Gorman, Adonis Bogris, Dimitris Syvridis, Sonali Dasgupta, Periklis Petropoulos and David J. Richardson, "*All-optical phase and amplitude regenerator for next-generation telecommunications systems*", Nature Photonics, **4**, 690–695 (2010).

3. Joseph Kakande, Radan Slavík, Francesca Parmigiani, Adonis Bogris, Dimitris Syvridis, Lars Grüner-Nielsen, Richard Phelan, Periklis Petropoulos and David J. Richardson, "*Multilevel quantization of optical phase in a novel coherent parametric mixer architecture*", Nature Photonics, **5**, 748–752 (2011).

4. Joseph Kakande, Adonis Bogris, Radan Slavík, Francesca Parmigiani, Dimitris Syvridis, Mats Sköld, Mathias Westlund, Periklis Petropoulos, and David J. Richardson, "*QPSK Phase and Amplitude Regeneration at 56 Gbaud in a Novel Idler-Free Non-Degenerate Phase Sensitive Amplifier*", OSA/OFC/NFOEC OMT4, (2011).

5. Joseph Kakande, Radan Slavík, Francesca Parmigiani, Periklis Petropoulos and David J. Richardson, "*All-Optical Processing of Multi-level Phase Shift Keyed Signals*", OSA/OFC/NFOEC OW1I.3, (2012).

6. Zuqing Zhu, Xiaoliang Chen, Fan Ji, Liang Zhang, Farid Farahmand, and Jason P. Jue, "*Energy-Efficient Translucent Optical Transport Networks With Mixed Regenerator Placement*", Journal of Lightwave Technology, **30** (19), 3147-3156 (2012).

7. P. Minzioni, V. Pusino, I. Cristiani, L. Marazzi, M. Martinelli and V. Degiorgio, "*Study of the Gordon–Mollenauer Effect and of the Optical-Phase-Conjugation Compensation Method in Phase-Modulated Optical Communication Systems*", IEEE Photonics Journal, **2** (3), 284-291 (2010).

8. D. Lavery, C. Behrens and S. J. Savory, "*A Comparison of Modulation Fortmats for Passive Optical Networks*", Optics Express, **19** (26), B836-B841, (2011)

9. K. Cvecek, K. Sponsel, G. Onishchukov, B. Schmauss, and G. Leuchs, "*Phase-preserving amplitude regeneration for a WDM RZ-DPSK signal using a nonlinear amplifying loop mirror*", IEEE Photonics Technology Letters, **19** (3), 146-148 (2007).

10. Xiang Liu, A. R. Chraplyvy, P. J. Winzer, R. W. Tkach and S. Chandrasekhar, "*Phase-conjugated twin waves for communication beyond the Kerr nonlinearity limit*", Nature Photonics, **7**, 560–568 (2013).

11. Jeng-Yuan Yang, Morteza Ziyadi, Youichi Akasaka, Salman Khaleghi, Mohammad R. Chitgarha, Joe Touch and Motoyoshi Sekiya, "*Investigation of Polarization-Insensitive Phase Regeneration Using Polarization-Diversity Phase-Sensitive Amplifier*", ECOC P3.07, (2012).

12. B. Stiller, G. Onishchukov, B. Schmauss and G. Leuchs, "*8-QAM regeneration using a phase-sensitive amplifier with dual-conjugated pumps*", CLEO Munich CI-P.14 (2013).

13. S. Sygletos, P. Frascella, S. K. Ibrahim, L. Grüner-Nielsen, R. Phelan, J. O'Gorman, and A. D. Ellis, "A practical phase sensitive amplification scheme for two channel phase regeneration", Optics Express, **19** (26), B938-B945 (2011).

14. K.J.Lee, F.Parmigiani, S.Liu, J.Kakande, P.Petropoulos, K.Gallo, D.J.Richardson, "Phase sensitive amplification based on quadratic cascading in a periodically poled lithium niobate waveguide", Optics Express **, 17** (22) , 20393-20400 (2009)

15. Takeshi Umeki, Masaki Asobe and Hirokazu Takenouchi, "*In-line phase sensitive amplifier based on PPLN waveguides*", Optics Express, **21** (10), 12077-12084 (2013).

16. Rene´-Jean Essiambre, Gerard J. Foschini, Gerhard Kramer, and Peter J. Winzer, "*Capacity limits of information transport in fiber-optic networks*", Physical Review Letters, **101**, 163901 (2008).

17. K. Thyagarajan and B. P. Pal, "*Modeling dispersion in optical fibers: applications to dispersion tailoring and dispersion compensation*", Journal of Optical and Fiber Communications Reports, **4** (3), 173–213 (2007).